ESRF	**Experiment title: One-dimensional confinement of plasmons in carbon nanotubes**	**Experiment number**: He-3037
Beamline: ID16	**Date of experiment**: from: 17.06.2009 to: 23.06.2009	**Date of report**: 28.08.2009
Shifts: 18	**Local contact(s)**: Simo Huotari	*Received at ESRF:*

Names and affiliations of applicants (* indicates experimentalists):

C. Kramberger*, T. Pichler,
University of Vienna, Faculty of Physics, Strudlhofgasse 4, A-1090, Vienna, Austria

E. Einarsson*, S. Maruyama,
The University of Tokyo, Department of Mechanical Engineering, 7-3-1 Hongo, Bunkyo-ku, Tokyo 113-8656, Japan

Report:

We used Beamline ID16 to investigate the electronic loss-function of oriented samples of carbon nanotubes by means of inelastic x-ray scattering (IXS). The low density samples consist predominantly of well separated small bundles formed by 3 to 7 individual single walled carbon nanotubes, that are glued together by Van der Waals forces and have a net alignment perpendicular to the films surface. Such films of vertically aligned SWNT are referred to as VA-SWNT. The cross sections of electron energy loss spectroscopy (AR-EELS) and IXS scale with $1/q^2$ and q^2 according to Rutherford and Thomson scattering, respectively. Preceding AR-EELS studies did reveal localized and delocalized plasmons in the loss-function of this peculiar one-dimensional meta-material. Delocalized plasmon are dispersive and propagate along the axis while localized modes do not show any dispersion. In AR-EELS experiments only near normal transmission and relatively small momentum transfers q are accessible. IXS can easily overcome these limitations because it benefits from larger momentum transfers and it may either be performed in forward or backscattering geometry. Because of the very different transmittance of an electron beam versus an x-ray beam, the VA-SWNT film thicknesses for EELS and IXS were choosen to be 5 µm and 100 µm. Just as in transmission electron microscopy (TEM) or AR-EELS the otherwise freestanding nanotube films were supported by standard copper grids. We found that the "one thick film approach" can indeed provide a satisfactory countrate for IXS, but only in backscattering geometry. In view of the utterly different requirements regarding sample thicknesses of IXS and AR-EELS we achieved during He-3073 to demonstrate that VA-SWNT allow to combine and also quantitatively compare AR-EELS and IXS to one another.

Figures 1 and 2 show the dispersion of the on-axis π and σ plasmon. The dispersions are archetypical for all sp² carbon like graphite, our sparse VA-SWNT or bulk SWNT material.
Bulk graphite confirms an excellent quantitative match between the two completely independend loss-functions (viz. their dispersions) obtained either by AR-EELS or IXS. respectively. Hence, the offset in the dispersion of the first and second batch of VA-SWNT can be clearly assigned to variations in the density. Bulk SWNT, and either batch of VA-SWNT, each has a different density. The densities result in a different strength of dielectric screening and accordingly different upshifts of the plasmon energies. The density of the 100 µm thick films is apparently three to four times higher than that of the just 5 µm thick nanotubes films but still far below that of graphite.
An interesting observation is made regarding the plasmon dispersions at different densities. The π plasmon of bulk SWNT (1.3 g/cm³) converges above 0.5 $\AA^{-1}$ towards the π plasmon of isolated VA-SWNT (0.05 g/cm³). The same behavior is seen for the respective σ plasmons. The regions of interest are highlighted by tilted green ovals in Figs. 1&2. The σ plasmons of bulk graphite (2.3 g/cm³) and isolated VA-SWNT (0.18 g/cm³) converge only above 2 $\AA^{-1}$, which is highlighted by a horizontal oval in Fig. 2. We link the convergence of plasmons from different densities at sufficiently high q to the fade out of dielectric screening, that decays like the Coulomb interaction with $1/q^2$. In this regime the loss-function is no longer made of collective plasmons, but it is entirely built up from electronic single particle excitations.
The present findings do quantitatively confirm that for solids the same loss-function may indeed be probed either by AR-EELS or IXS. Regarding VA-SWNT this congruency can be confirmed for the dispersive on-axis plasmons, but the localized modes are an open issue. Due to the complementary q dependence the two methods are a powerful combination for tracing electronic excitations across a wide range of momentum transfers. The various densities investigated here allow us to identify and even quantify the regime of the fully intrinsic electronic excitation spectrum for all sp² carbon.

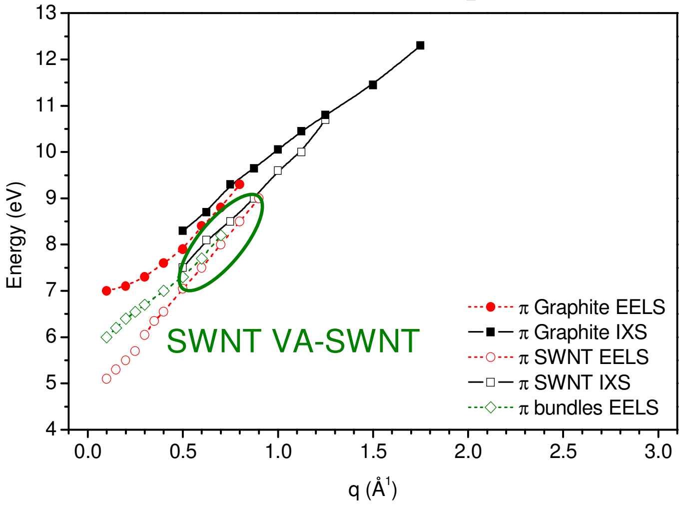

Fig. 1 Dispersion of the π plasmons of graphite and SWNT measured by IXS and EELS. Different densities converge in the oval.

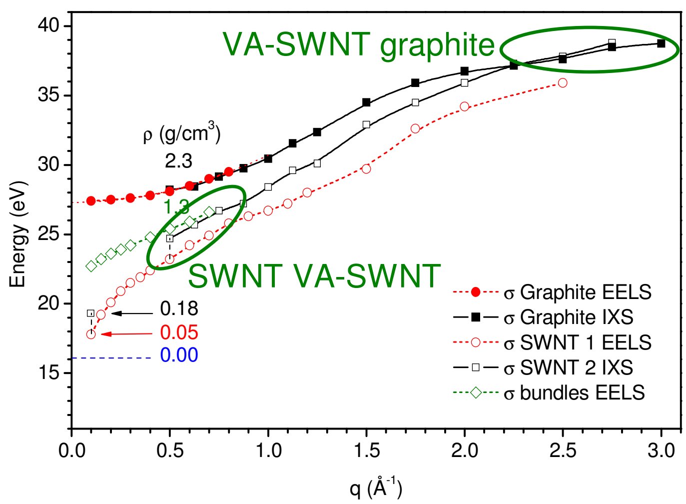

Fig. 2 Dispersion of the σ plasmons of graphite and SWNT measured by IXS and EELS. Different densities converge in the ovals.

.